Computational Materials Science 158 (2019) 389–397

Contents lists available at ScienceDirect

Computational Materials Science

journal homepage: www.elsevier.com/locate/commatsci

Assessment of discrete breathers in the metallic hydrides

Vladimir Dubinko[a,*], Denis Laptev[b], Dmitry Terentyev[c], Sergey V. Dmitriev[d,e], Klee Irwin[f]

[a] NSC Kharkov Institute of Physics and Technology, Kharkov 61108, Ukraine
[b] B. Verkin Institute for Low Temperature Physics and Engineering, Kharkov 61103, Ukraine
[c] SCK•CEN, Nuclear Materials Science Institute, Boeretang 200, Mol, 2400, Belgium
[d] Institute for Metals Superplasticity Problems, Ufa 450001, Russia
[e] National Research Tomsk State University, Tomsk 634050, Russia
[f] Quantum Gravity Research, Los Angeles, USA

ARTICLE INFO

Keywords:
Discrete oscillations
Hydride
Molecular dynamics

ABSTRACT

Computational assessment of the discrete breathers (also known as intrinsic localised modes) is performed in nickel and palladium hydrides with an even stoichiometry by means of molecular dynamics simulations. The breathers consisting of hydrogen and metallic atoms were excited following the experience obtained earlier by modelling the breathers in pure metallic systems. Stable breathers were only found in the nickel hydride system and only for the hydrogen atoms oscillating along ⟨1 0 0⟩ and ⟨1 1 1⟩ polarization axes. At this, two types of the stable breathers involving single oscillating hydrogen and a pair of hydrogen atoms beating in antiphase mode were discovered. Analysis of the breather characteristics reveals that its frequency is located in the phonon gap or lying in the optical phonon band of phonon spectrum near the upper boundary. Analysis of the movement of atoms constituting the breather was performed to understand the mechanism that enables the breather stabilization and long-term oscillation without dissipation its energy to the surrounding atoms. It has been demonstrated that, while in palladium hydride, the dissipation of the intrinsic breather energy due to hydrogen-hydrogen attractive interaction occurs, the stable oscillation in the nickel hydride system is ensured by the negligibly weak hydrogen-hydrogen interaction acting within a distance of the breather oscillation amplitude. Thus, our analysis provides an explanation for the existence of the long-living stable breathers in metallic hydride systems. Finally, the high energy oscillating states of hydrogen atoms have been observed for the NiH and PdH lattices at finite temperatures which can be interpreted as a fingerprint of the finite-temperature analogues of the discrete breathers.

1. Introduction

Discrete breathers (DB) or intrinsic localized modes (ILM) are the spatially localized and periodic in time nonlinear excitations of the lattices [1–4]. The two critical components such as nonlinearity and discreteness must combine to make a DB to exist. Nonlinearity allows the strongly excited localized modes to have a fundamental frequency outside the spectrum of small amplitude oscillations, and the finite extend of the spectrum in a discrete system allows all higher harmonics of the DB also to lie outside the linear spectrum. The absence of interference of the DB frequencies with the lattice phonons prevents the resonances that, in general, destroy the continuum breathers in non-integrable systems.

The majority of pioneering theoretical studies on DBs dealt with the idealized one- or two dimensional nonlinear lattices of coupled oscillators interacting via simplified pairwise potentials with polynomial nonlinearity. It has been shown that integrable nonlinear lattices, such as Hirota [5] or Ablowitz-Ladik lattice [6,7], support exact solutions in the form of spatially localized excitations. For instance, Bogdan has obtained the exact DB solution for the Hirota lattice equation [8]. In further publications the exact Hamiltonian dynamics [9] and pair interactions processes [10] of these excitations were investigated analytically. However a number of exactly solvable and physically important nonlinear discrete lattices is rather small. That is why it was important to prove rigorously the existence and stability of DB in non-integrable nonlinear chains [11–13].

The role of DBs has been extensively discussed in the fields of nonlinear optics [14,15], superconducting Josephson junctions [16,17], electric circuit arrays [18,19], micromechanical and macromechanical cantilever arrays [20,21], mechanical systems [22,23], granular crystals [24], etc.

Discrete breathers in crystalline solids have been actively studied in

* Corresponding author.
E-mail address: vlad@quantumgravityresearch.org (V. Dubinko).

https://doi.org/10.1016/j.commatsci.2018.11.007
Received 7 August 2018; Received in revised form 1 November 2018; Accepted 2 November 2018

recent years in relation with their physical and mechanical properties [25,26]. The atomic-scale nature of DBs, quantum effects behind and scarcity of events make the observation and experimental registration of these excitations challenging. Nevertheless, there are a number of experiments demonstrating the existence of DBs in different crystals. In the experiments with the nonlinear halide-bridged mixed-valence quasi-one-dimensional transition metal complex PtCl [27] a strong evidence for the existence of DBs has been found by measuring resonance Raman spectra. The redshift in the resonances indicated the localized excitation of Pt−Cl bonds. Manley et al. [28,29] have reported an experimental observation of gap DBs (i.e. DBs with the frequency laying in the gap of the phonon spectrum of bi-atomic system) in thermodynamic equilibrium in NaI crystal. In a series of experimental works, evidence supporting existence of DBs in alpha-uranium has been obtained [30–32]. Recent reviews [33–35] summarize the results of the theoretical and experimental investigations and the molecular-dynamics simulations of DBs in two- and three-dimensional crystals.

Particular importance attributed to DBs is defined by their potential role in determining rates of non-equilibrium processes in real material (e.g. chemical diffusion, catalysis, defect migration and annealing, activation of dislocations and other atomic-scale mechanisms) [36–38]. DBs can enhance heat capacity by storing some energy [30]. They can also reduce thermal conductivity by scattering phonons [39]. On the other hand, mobile DBs can enhance heat conductivity by transporting energy [31].

In the recent years, DB-mediated effects in solid state physics and materials science have been the focus of a rapidly growing number of studies based on more realistic atomistic models of crystals. With the appearance of powerful computational methods, the research focus has shifted to simulations in 3D lattices using realistic many-body potentials and investigating properties of breathers at finite temperature [40–42] or in non-ideal crystals containing lattice defects [43]. Molecular dynamics (MD) was applied to study breathers not only in single-atomic systems like covalent silicon and diamond [44,45], pure metals [43,46–50] but also in the ordered alloys [51–53], as well as in ionic crystals with NaCl structure [54–57]. Not only MD [58–64] but also *ab initio* simulations support existence of DBs in 2D crystalline structures such as graphene and graphane [65,66].

The existence of breathers in PdH and NiH systems may have a number of important applications for the hydrogen technology. Hydrogenation is a chemical reaction between molecular hydrogen and another compound or element, usually in the presence of a *catalyst* such as nickel or palladium. There is no single theory of catalysis, but only a series of principles to interpret the underlying processes. An important parameter of the reaction kinetics is the activation energy, i.e. the energy required to overcome the reaction barrier. The lower is the activation energy, the faster the reaction rate, and so a catalyst may be thought to reduce somehow the activation energy. Dubinko et al [36–38] have suggested that DBs arising in the vicinity of a reaction cite result in a time-periodic modulation of the potential landscape, which can be described by a combination of time-periodic modulation of the activation barrier height and shape. The height modulation effect was shown to result in a drastic acceleration of escape from the potential well driven by thermally-activated 'jumps' over the reaction barrier [36,37]. The shape modulation effect was shown to result in a strong acceleration of tunnelling through the potential barrier at sufficiently low temperatures, where the reaction rates are controlled by quantum rather than by thermal **fluctuations** [38]**. These results** support the concept of DB mediated catalysis at both high and low temperatures, which shows the need for more detailed atomistic modeling of DBs in various physical systems.

Here, we investigate the existence of DBs in the nickel and palladium hydrides systems by means of modern atomistic computational tools involving usage of *ab initio*-derived many body interatomic potentials, which accurately reproduce a number of features of the studied hydrides. By performing MD simulations at zero and finite temperature we investigate the existence of breathers and their characteristics regarding the location of their frequencies in the phonon spectrum. As this is the first step, we take an idealized structure of the perfectly stoichiometric hydrides with chemical formulas NiH and PdH having the lattice structures equivalent to NaCl ionic crystal.

2. Computational details

The assessment of DB's characteristics in PdH and NiH systems has been performed using classical MD simulations in 3D periodic crystals. The PdH and NiH structures were generated using Latgen code supplied with LAMMPS package [67]. We have modelled the stoichiometric hydrides where fcc hydrogen sub-lattice occupies octahedral positions in the fcc metallic (palladium or nickel) sub-lattice.

MD simulations were carried out by employing the many-body type interatomic potentials derived on the basis of available experimental data and *ab initio* results. The PdH and NiH potentials were taken from [68] and [69], respectively. These potentials were developed to account for specific properties of H in Ni and Pd crystals, overall showing a good agreement with available experimental and *ab initio* data as what concerns basic properties. In this work we did not involve density functional theory calculations as yet, because it imposes high computational demand, given that a high number of various configurations must be studied. MD simulations with realistic many-body potentials are known to be a good compromise to encompass the research, while *ab initio* methods can be applied in future to validate the MD results.

MD simulations were done in the virtual 3D-periodic crystals with three principal axes oriented along the ⟨1 0 0⟩, ⟨0 1 0⟩ and ⟨0 0 1⟩ directions, respectively. The size of the MD supercell was chosen to be 10, 10, and 10 atomic planes along x, y and z. Such MD box is sufficiently large to avoid the self-interaction of a highly localized DB via periodic boundaries.

A DB was created in the crystal by setting an initial displacement along a selected close packed direction, where the breather is mostly expected to be stable, following the example of earlier studies in pure metals [46–50]. The key feature of the excitation of the breather is the choice of the initial displacement direction and selection of configuration involving one, two or a higher number of initially excited atoms. The central offset displacement will be referred in the following as d_0. Its variation determines the DB amplitude and frequency and, ultimately, its oscillating lifetime. In practice, such an initial condition of the DB excitation corresponds to the recoil processes which can be the result of exposure to high-energy particle beam or a shock wave.

Prior to initiating a DB a full relaxation to zero pressure and zero temperature was achieved by the conjugate gradient method. All initial velocities of atoms were set to zero. Two types of breathers were probed in this study. The first type implies the excitation of a single atom, such that the oscillation of a hydrogen atom between two metallic atoms realizes. Thus, such configuration is referred to as "M−H−M" breather. A schematic representation of its initial configuration is shown in Fig. 1. One hydrogen atom, originally located in the centre of the picture, is displaced to the left. In what follows, as we shall discuss characteristics of DBs, the analysis of the distance between the H atom constituting the DB and hydrogen/metallic nearest neighbour atom will be performed. These two distances are shown in Fig. 1 as r(H−H) and r(H−M). Fig. 2 shows the initial configuration of the H−M−H breather which consists of H1 and H2 atoms beating in the antiphase and being separated by M2 atom.

Each type of breather was excited by gradually increasing d_0 up to the situation when the point defect was generated as a result of the evolution of atomic motion. In order to quantify characteristics of stable DBs, the profiles of atomic positions and potential energy function of atoms constituting the breather were analyzed. The time evolution of the displacement of H and M atoms (constituting the breather) from their equilibrium positions was used to define the eigen frequencies of the DBs. To complete the analysis of the breather characteristics, the

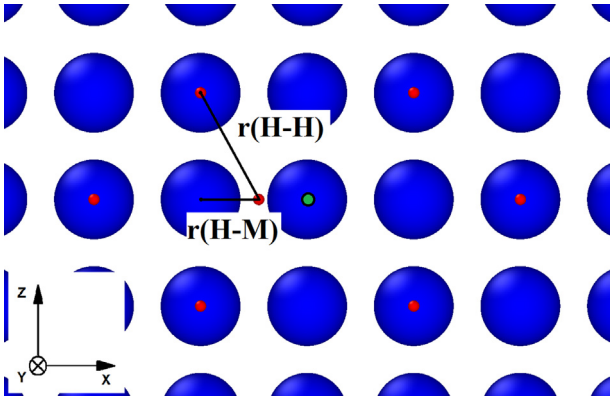

Fig. 1. Schematic representation of the initial configuration of the M−H−M type breather. The length of the H−M and H−H bond, shown respectively as r (H−M) and r(H−H), is analysed during the simulation. Large blue balls showing metallic atoms and small red balls showing hydrogen atoms are drawn at a scale of ionic ratio for nickel (Ni) and hydrogen (H). Green small ball in the center represents the equilibrium position of the H atom.

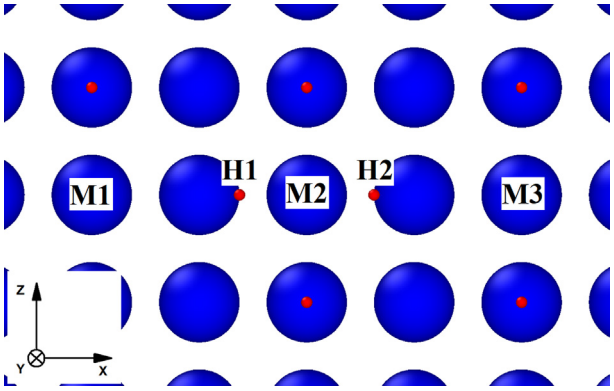

Fig. 2. Schematic representation of the initial configuration of the H−M−H type breather. Blue large balls showing metallic atoms and red small balls showing hydrogen atoms are drawn at a scale of ionic ratio for nickel (Ni) and hydrogen (H).

phonon density of states for the PdH and NiH systems were derived using the procedure proposed in [70]. In [70], the methodology to calculate the phonon dispersion of a crystal using molecular dynamics simulations is proposed and implemented as an open source routine to be plugged to LAMMPS code. The dynamical matrix is used to compute the phonon spectra by evaluating its eigenvalues. The dynamical matrix is constructed by recording the displacements of atoms during a representative MD run, making the use of the fluctuation–dissipation theory.

The finite temperature simulations were also performed to investigate potential existence of breathers at elevated temperature, following the methodology proposed in Refs. [40,41]. Those works exploited an idea of spatial and temporal temperature (i.e. atomic velocity) analysis. From such a combined analysis, the breathers were deduced on the basis of a specific numerical criterion which reflects local temperature within a certain timespan. In this case, the MD simulations of PdH and NiH at finite temperature using NVE micro-canonical ensemble were carried at the temperature of 300 K. From the finite temperature simulations, the velocity profile of all the atoms in the system was analysed and post-processed to deduce the presence of the breather according to the definition introduced in [41].

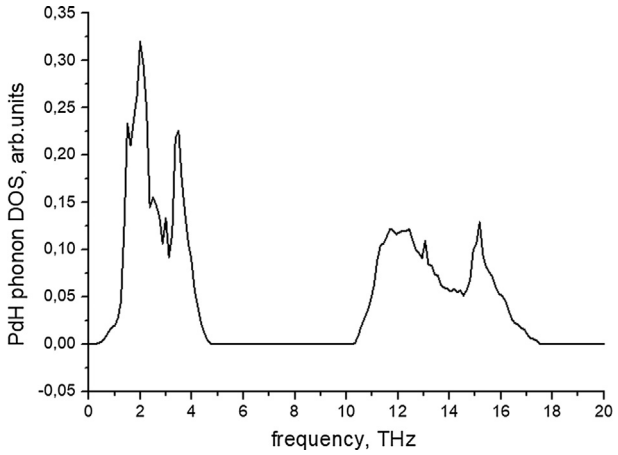

Fig. 3. Phonon density of states for the PdH lattice.

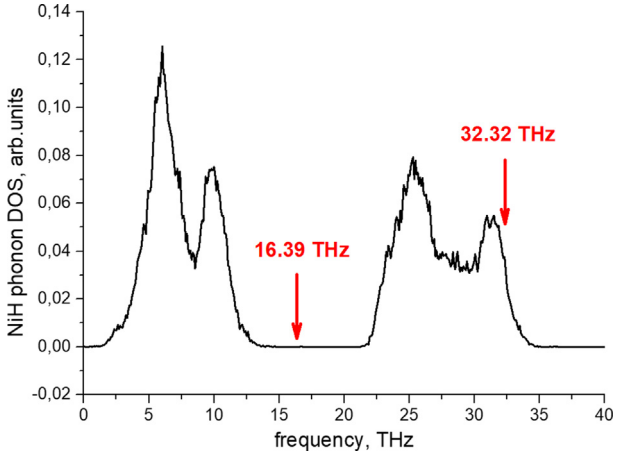

Fig. 4. Phonon density of states for the NiH lattice. The frequency of stable (i.e. long-living) breathers found in this work are indicated on the figure by red arrows.

3. Results

3.1. Modeling discrete breathers at zero temperature

The phonon density of states for PdH and NiH systems, obtained at low temperatures (1 K), are presented in Figs. 3 and 4, respectively. It can be seen that for PdH lattice the gap in the phonon spectrum is located in the frequency band of 4.7–10.4 THz, and the high frequency part extends up to 17.5 THz. For the NiH lattice there is a gap in the 13.5–21.5 THz frequency interval and the upper edge of the phonon spectrum is 34.5 THz. Thus, we expect to observe breathers in PdH and NiH lattices with frequencies either lying in the gap or exceeding the upper limits of the phonon spectra.

As was explained earlier, the breathers with different polarization axes were excited by gradually increasing the initial displacement d_0, see Figs. 1 and 2. The general trend for the stability of the breather with increasing d_0, that was observed for all polarization axes, is presented in Fig. 5 by the example of the ⟨1 0 0⟩ H−M−H breather in Ni−H system. Supplementary material includes the animation of the atomic movement that realizes in each specific case presented in Fig. 5. If the excitation amplitude is too small, see Fig. 5(a), the H oscillation quickly decays and the DB energy is quickly dissipated to the surrounding atoms i.e. to the lattice. Given a sufficient offset displacement distance, the oscillation of H atom is stabilized after a short transient period. An example of the evolution of the atomic coordinates of five atoms forming the breather is shown in Fig. 5(b). It is seen that shortly after

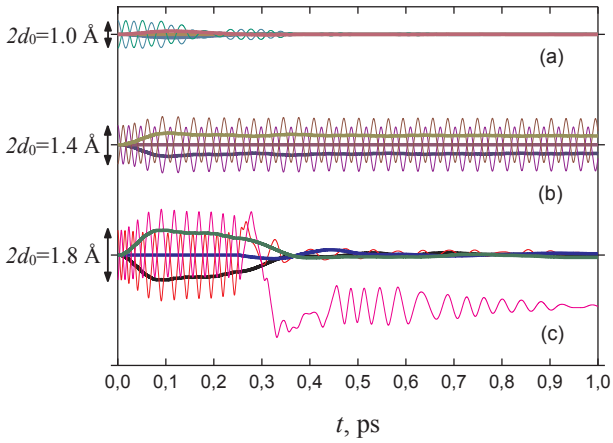

Fig. 5. Evolution of the displacement of atoms from their equilibrium positions for the case of H−M−H ⟨1 0 0⟩ breather in NiH system: (a) small (d_0 = 0.5 Å), (b) middle (d_0 = 0.7 Å) and (c) large (d_0 = 0.9 Å) initial displacement, see text for details. Thick/thin lines correspond to the Ni/H atoms displacements from the equilibrium positions. The arrows next to the ordinate show the absolute value of the atomic oscillation relative to the equilibrium position.

the breather is launched, the M1 and M3 metallic atoms bounding the oscillating H1 and H2 atoms slightly displace to extend a volume for the oscillating H atoms. Centers of vibration of the two H atoms vibrating out-of-phase also shift from the equilibrium positions. Then, the system comes to quasi-stationary motion and such a breather performs its stable oscillation up to 400 cycles of full vibration periods at nearly constant amplitude, without losing its energy. Analysis of the atomic motion shows that such a breather represents fully symmetric system where M2 (see Fig. 2) is the center of the symmetry. This long-living breather was analyzed in details to calculate the kinetic energy stored in this defect. The kinetic energy of the breather was calculated as the average kinetic energy of five atoms (two hydrogen and three metallic atoms) forming the breather. It was found that the kinetic energy of the breather shown in Fig. 5(b) is 1.23 eV.

Increasing the initial amplitude further leads to the displacement of H atom(s) from their original sites and subsequent creation of point defect(s). Such example is shown in Fig. 5(c), where one of H atoms is eventually displaced out of its original site. Thus, the excitation of the stable breather requires careful choice of d_0 as was originally anticipated.

The same type of calculations were repeated in the NiH for ⟨1 1 0⟩ and ⟨1 1 1⟩ polarization axes. It was found that depending on specific polarization axis, optimal d_0 and therefore resulting DB frequency differ. Moreover, for some of the polarization directions the excitation of both types of the breathers was not successful. Hence, depending on the polarization axis, different types of breathers may exist. Analysis of the oscillations of the long-living breathers in NiH system revealed that 16.39 and 32.32 THz are the frequencies of the most stable gap-type and high frequency type M−H−M breathers, respectively.

Several examples of the atomic oscillations, which were found to be the most stable, are provided for the ⟨1 0 0⟩ (Fig. 6), ⟨1 1 0⟩ (Fig. 7) and ⟨1 1 1⟩ (Fig. 8) polarizations of the M−H−M breathers, respectively. The animation of the atomic motion near the location of each of the breather, shown on those figures, is included in the supplementary material. An example of the high frequency M−H−M breather with ⟨1 0 0⟩ polarization axis is provided in Fig. 6, where the displacement of hydrogen from its initial position is shown as the function of time. By analyzing the atomic trajectory over the stable oscillation time interval, the following breather parameters were deduced: the oscillation amplitude is 1.05 Å, oscillation frequency is 32.32 THz, oscillation period 0.03 ps and lifetime is 8.3 ps, which is equivalent to 276 oscillation periods. Another example of the M−H−M breather, which was excited in ⟨1 0 1⟩ direction, is presented in Fig. 7. This breather decayed rather quickly within less than 1 ps, however, it is oscillation frequency is found to be 18.88 THz, thus it is the gap-type breather. The variation of d_0 did not result in the formation of any other stable breather configurations for this excitation direction. Changing the excitation direction to ⟨1 1 1⟩, we found a very stable M−H−M gap-type breather. The oscillation profile is given in Fig. 8, where we present the zoomed area for 1 ps simulation time span and 25 ps segment. This breather was seen to be stable for more than 100 ps. The resulting oscillation frequency is 16.39 THz and period 0.061 ps, proving that this is gap-type breather.

Repeating the same calculations in the PdH system did not result in the observation of stable oscillations. Figs. 9 and 10 show examples of the evolution of atomic oscillations in PdH lattice for the case of H−M−H and M−H−M breathers, respectively. Both figures demonstrate that irrespective of the polarization axis the oscillation is promptly extinguished. The same qualitative result was obtained for other excitation directions and various d_0.

One possible reason for the very short DB lifetime observed in our simulations for PdH is the use oversimplified initial conditions. As it has been pointed out, vibration of H atoms results in the displacement of the neighboring metallic atoms (see, e.g., Figs. 5 and 9). This displacement was not taken into account in setting up the initial conditions, and more sophisticated initial atomic setting might help for the DB to remain longer. It is clear that since Pd atom is nearly as twice heavier as Ni atom, the use of these simplified initial conditions for PdH system can be more problematic than for NiH.

To further rationalize the reasons for the difference in the oscillation behavior of atoms in nickel and palladium hydrides we calculated the effective potential pair profile for hydrogen-hydrogen and metal-hydrogen and calculated the interaction force for the M−H−M type DB polarized along ⟨1 0 0⟩ direction. This is shown in Figs. 11 and 12 for the NiH and PdH systems, respectively. Each figure contains the profile of the effective pair interaction force i.e. negative derivative of the effective pair potential. The effective pair potential is calculated using molecular static approach by moving an atom in the lattice, while keeping the surrounding neighbours constrained in their positions. The vertical lines labeled as $r^{M-H}_{min/max}$ and $r^{H-H}_{min/max}$ denote the minimum M−H/H−H distance which realizes as the breather oscillates in the steady-state mode, where M denotes nickel (Ni) or palladium (Pd). Given the spatial boundaries, specified by vertical lines on the figures, one can understand the evolution of the force acting on the oscillating H atom during the whole oscillation cycle of a DB. Positive (negative) force in Figs. 11 and 12 is repulsive (attractive).

Considering the case of the DB in NiH lattice (see Fig. 11). Note that within the span of H atom oscillation, the H−H interaction is negligibly weak as compared to the Ni−H interaction. In the case of DB in PdH lattice (Fig. 12), H−H interaction is not weak. Stronger interaction between nearest H atoms can be the reason for delocalization of the DB in PdH crystal. Of course, the measured interaction forces and the behavior of the DB in general is being determined by the empirical potential applied in this work.

Thus, the stability of a DB oscillation process in NiH can be qualitatively explained by the short-range H−H interaction in this lattice. Contrary to that, the long-range H−H interaction in Pd−H lattice results in formation of less localized DB whose excitation requires the use of more sophisticated initial conditions.

3.2. Modeling discrete breathers at finite temperature

The results of the simulations of the hydride lattices at finite temperature are presented in this section. As was explained in Section 2, the finite temperature simulations were performed to analyze the kinetic energy of randomly sampled hydrogen and metallic atoms with the purpose to reveal the existence of high kinetic energy particles observable for the time period comparable to several oscillations of the breather. The general methodology regarding the lattice thermalization and registration of the thermal spikes was adopted from Refs. [40,41].

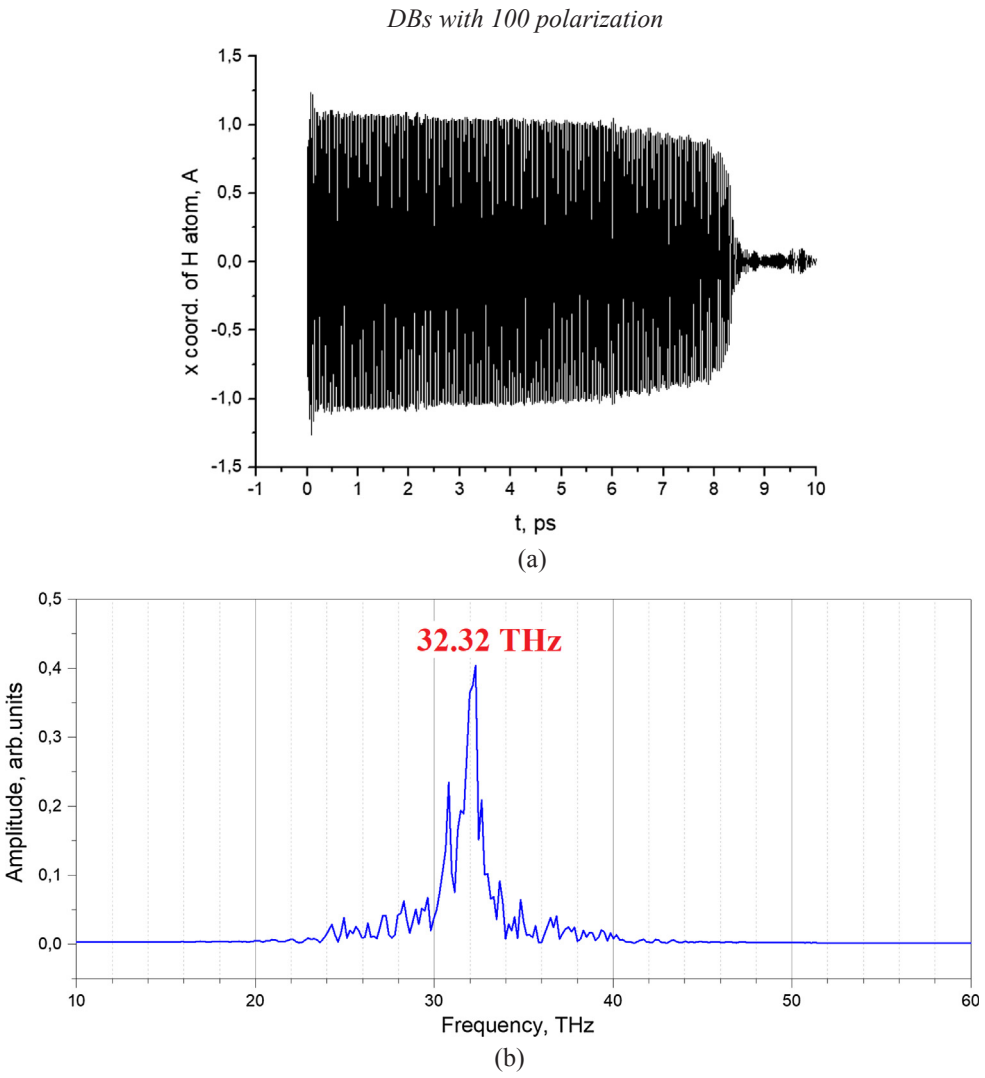

Fig. 6. (a) Oscillation of a hydrogen atom forming the M−H−M ⟨1 0 0⟩ breather in NiH lattice initiated with $d_0 = 0.84$ Å. The resulting oscillation amplitude is 1.05 Å, oscillation frequency is 32.32 THz, oscillation period is 0.03 ps and lifetime is 8.3 ps, which is equivalent to 276 oscillation periods. (b) Fourier spectrum constructed using the trajectory presented in Fig. a. The position of the peak corresponds to the oscillation frequency of 32.32 THz.

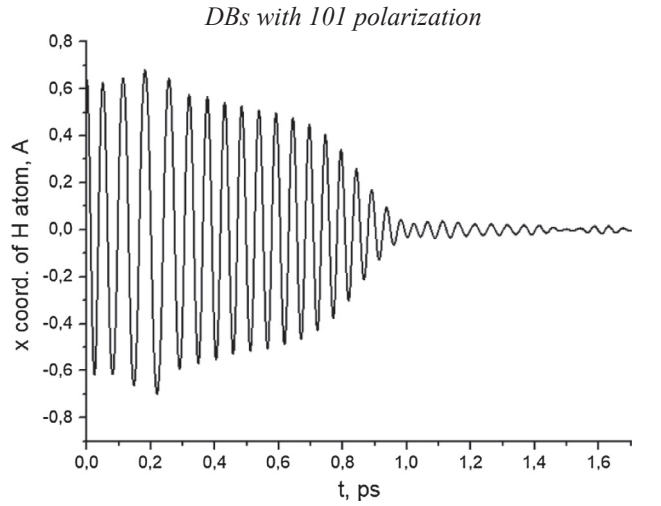

Fig. 7. Oscillation of a hydrogen atom forming the M−H−M ⟨1 0 1⟩ breather in NiH lattice with $d_0 = 0.9$ Å. The resulting oscillation amplitude is 0.5 Å, oscillation frequency is 18.88 THz, oscillation period is 0.053 ps and lifetime is 0.86 ps, which is equivalent to 15 oscillation periods.

Firstly, the system is thermalized using Langevin algorithm, introduced in the LAMMPS. Once the thermal equilibrium at a desired temperature is reached, the atoms are self-evolving in the NVE ensemble and the measurement of the kinetic energy is performed.

The distribution of the kinetic energy (in reduced units) of a randomly selected H and metallic atoms across the simulation timespan of 30 ps is shown in Figs. 13(a and b) and 14(a and b) for NiH and PdH lattices, respectively. The kinetic energy of the atom is scaled by the average kinetic energy of the system which equals to the total kinetic energy of the lattice divided by a total number of atoms in the lattice and averaged over the timespan of 100 fs. This characteristic time interval is comparable to several periods of the DB oscillation as measured in simulations at 0 K in NiH lattice. Thus, each point on these figures is obtained by averaging the kinetic energy of the atom over the three consecutive time segments and scaled by the average kinetic energy of the system. The net value of such distribution is unity, however, during the simulation run one can see that both H and metallic atoms spend several oscillation periods with the energy significantly exceeding the average kinetic energy of the system (i.e. by a factor 2–3), which can be interpreted as a signature of the existence of short-living breathers.

The post processing of the curves shown in Figs. 13(a and b) and 14(a and b) was made to identify the existence of the short-living oscillations with the atomic kinetic energy exceeding the average kinetic energy of the system by at least a factor of 2. Detailed analysis of these

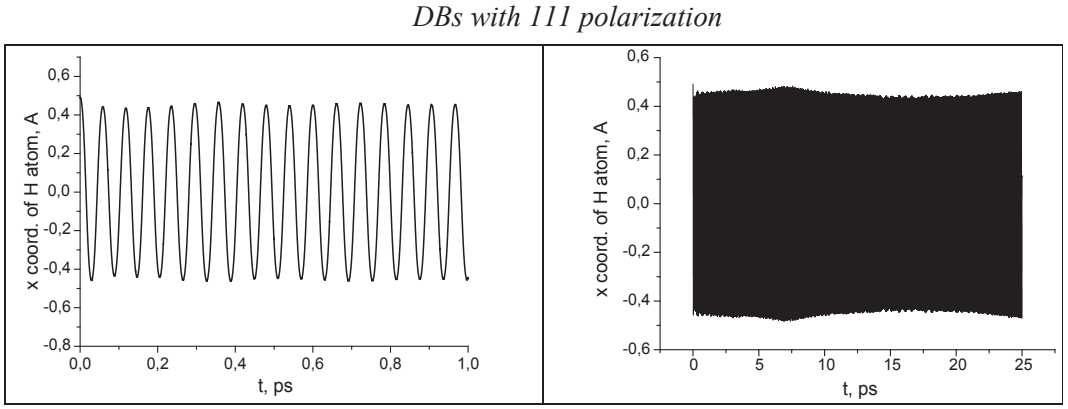

Fig. 8. Oscillation of a hydrogen atom forming the M−H−M ⟨1 1 1⟩ breather in NiH lattice with $d_0 = 0.85$ Å. The resulting oscillation amplitude is 0.79 Å, oscillation frequency is 16.39 THz, oscillation period is 0.061 ps and lifetime is higher than 100 ps–1640 oscillation periods (the simulation run was stopped before the breather oscillation decayed).

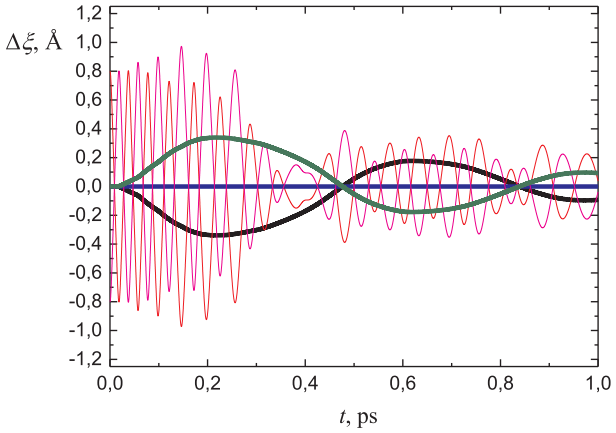

Fig. 9. Evolution of the displacement of atoms from their equilibrium positions for the case of H−M−H ⟨1 0 0⟩ breather with $d_0 = 0.8$ Å in PdH system. Thick/thin lines correspond to the Pd/H atoms displacements from the equilibrium positions.

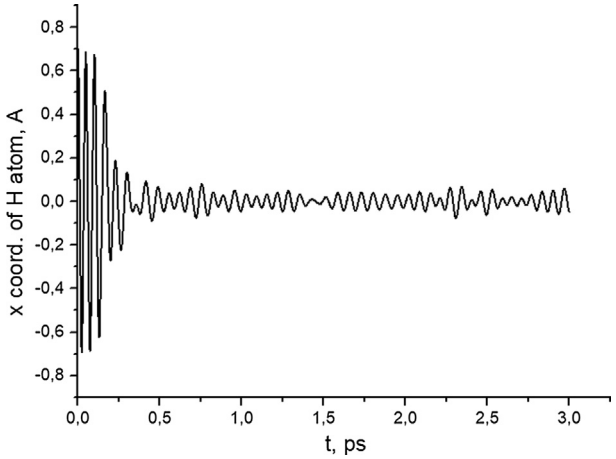

Fig. 10. Evolution of the displacement of H atom from its equilibrium position for the case of M−H−M ⟨1 0 0⟩ breather with $d_0 = 0.7$ Å in PdH system.

distributions reveals the high energy oscillations that occur regularly over the time span of about 1–2 ps. We observed that the high temperature spikes sustain within during about three oscillation periods. Such high temperature spikes occur with a frequency of 10–50 periods i.e. each 1–5 ps. The observation of the high energy spikes (or bursts), such as shown in Figs. 13 and 14(a and b), was also confirmed by

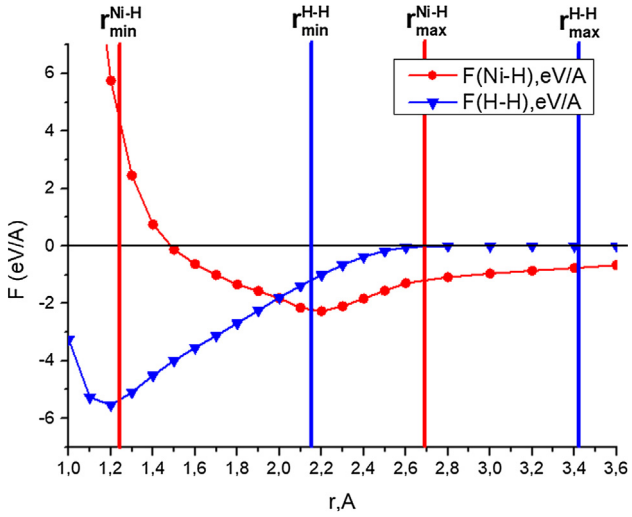

Fig. 11. Interaction force of the Ni−H and H−H atomic pairs as a functions of the distance between the atoms embedded in NiH lattice for the case of M−H−M DB polarized along ⟨1 0 0⟩ direction. Negative values correspond to the attractive interaction, while the positive values to the repulsive interaction.

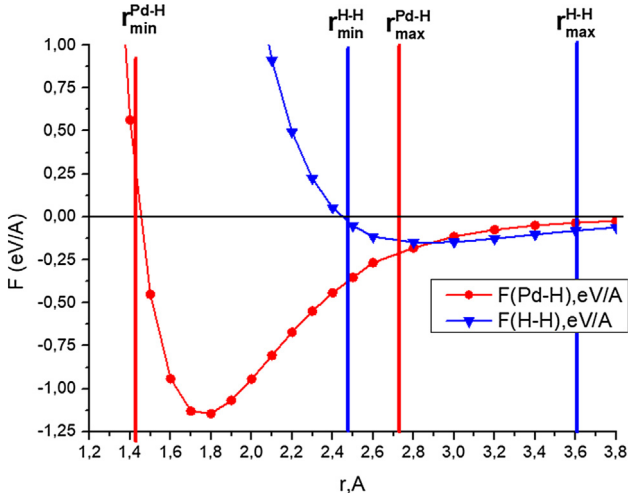

Fig. 12. Interaction force of the H-Pd and H−H atomic pairs as a functions of the distance between the atoms embedded in PdH lattice for the case of DB polarized along ⟨1 0 0⟩ direction. Negative values correspond to the attractive interaction, while the positive values to the repulsive interaction.

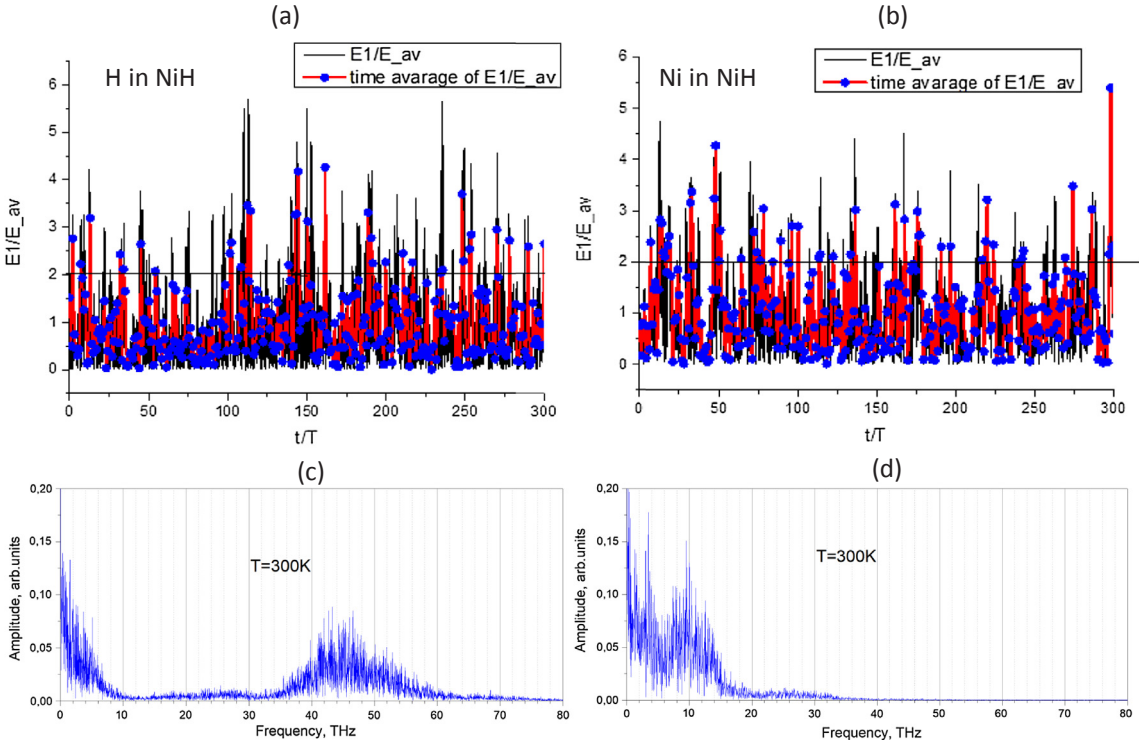

Fig. 13. Distribution of the normalized kinetic energy of a randomly selected (a) H atom and (b) Ni atom in the nickel hydride lattice normalized over the average kinetic energy of the system and averaged over the time segment of $T = 100$ fs. Fourier spectra of the same (c) H and (d) Ni atoms. MD simulations are performed at temperature of 300 K.

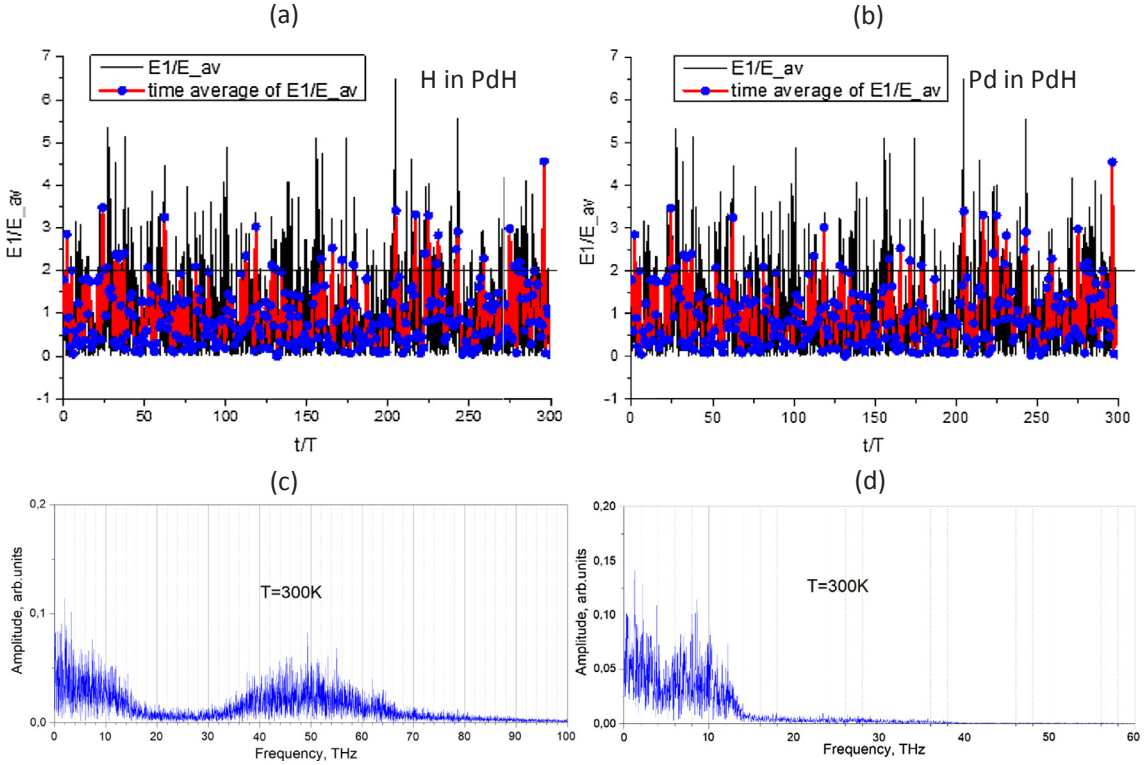

Fig. 14. Distribution of the normalized kinetic energy of a randomly selected (a) H atom and (b) Pd atom in the palladium hydride lattice normalized over the average kinetic energy of the system and averaged over the time segment of $T = 100$ fs. Fourier spectra of the same (c) H and (d) Pd atoms. MD simulations are performed at temperature of 300 K.

selection of other atoms from the same simulation run. Thus, the distributions shown are statistically significant results.

Comparison of the results presented for NiH and PdH shows that the occurrence of high temperature spikes is qualitatively observed in both lattices. However, a closer look reveals that the amplitude of the spikes in PdH system is systematically lower than that in the NiH system. To provide an insight in the oscillation process, we have constructed Fourier spectra for the same atoms which were used to plot the reduced average kinetic energy. Figs. 13 and 14(c and d) collect those Fourier spectra for Ni−H and Phd−H systems, respectively. As one can see, H atoms oscillate with the frequency corresponding to both optical and acoustic mode. Note that only in NiH lattice, one can reveal a weak peak in the gap of the phonon density of states, which can possibly explain more intensive (in terms of kinetic energy) bursts in Ni−H compared to Pd−H system. The vibration of metallic atoms occurs only in the acoustic mode in both systems and no specific difference between the two hydrides can be revealed.

At this stage, the results presented in this section are still preliminary and more in-depth investigation by applying integrated trajectory-energy-time correlation analysis is currently ongoing in order to formulate more concrete numerical criteria for the definition of breathers at elevated temperature and rationalize the origin of the observed bursts.

4. Summary and conclusions

In this work, we have analysed the existence of discrete breathers in two important metallic hydride systems, namely NiH and PdH. The assessment was performed by employing 3D atomistic simulations with realistic many-body interatomic potentials, developed to account for specific properties of hydrogen in these metallic lattices. The simulations were performed in the fully relaxed lattice at initial temperature of zero Kelvin, and at elevated temperature using conventional MD simulations. The simulations performed at zero temperature were used to explore typical characteristics of the hydrogen breathers by varying the polarization axis, intrinsic oscillation energy and hydrogen-metal configuration defining the breather structure (i.e. H−M−H or M−H−M type of oscillation). Parametric study was applied to scan a large range of the excitation amplitudes (related to the intrinsic oscillation energy) to deduce the most stable breathers, where stability refers to the number of oscillations prior the breather is absorbed by the lattice. To classify the type of the breather, the phonon density of states for both hydride systems were calculated using the selected set of potentials. By comparing the frequency of the breathers as measured in zero temperature simulations with the density of states, we conclude that both gap-type and high frequency breathers exist in NiH system. However, by applying the methodology to PdH system, we could not excite a long-lived breather of either type. Following the results of the simulations at zero Kelvin, we have constructed the diagrams of the effective pair interaction profiles and analysed the forces acting on atoms constituting the breathers in PdH and NiH systems. Such analysis was applied to rationalize the origin of the stability of the long living breathers as well as to clarify the difference in the breather characteristics in NiH and PdH systems. Finally, the MD simulations at elevated temperatures were performed to identify fingerprints of high temperature breathers by analysis of the kinetic energy distribution functions in accordance with the earlier studies performed on mono- and bi-atomic systems of another compounds.

On the basis of the results and discussion provided above it is possible to state the following:

(i) Both, gap-type and high frequency breathers are discovered in the nickel hydride system using classical molecular dynamics simulations with reliable many-body interatomic potentials. Depending on the polarization axis the breather has the frequency that falls in the gap of the phonon spectrum, or its frequency is near the upper phonon band edge.
(ii) Application of the same methodology to PdH system did not result in the observation of the breathers of either kind. The reasons for that discrepancy between two systems were rationalized on the basis of the analysis of the effective pair interaction of H−H and H−M pairs as they perform oscillation in the just excited breather. The origin of the stability of the breather in NiH is explained by short-range H−H interaction, which is not the case of the PdH system.
(iii) Finite temperature simulations have revealed the occurrence of short-living high energy oscillations, which could be attributed to the presence of so-called high temperature breathers following the definition introduced in [41]
(iv) With respect to the potential technological applications these results are important because breathers in PdH and NiH systems can act as catalysts of various reactions of technological importance [36–38,71–73].

CRediT authorship contribution statement

Vladimir Dubinko: Writing - original draft, Conceptualization, Project administration. **Denis Laptev:** Investigation, Validation, Visualization. **Dmitry Terentyev:** Writing - original draft, Software. **Sergey V. Dmitriev:** Writing - review editing, Formal analysis. **Klee Irwin:** Writing - review editing, Project administration, Funding acquisition.

Acknowledgements

S.V.D. thanks the Russian Science Foundation, grant no. 16-12-10175, for the financial support.

Data availability

The raw/processed data required to reproduce these findings cannot be shared at this time as the data also forms part of an ongoing study.

Appendix A. Supplementary material

Supplementary data to this article can be found online at https://doi.org/10.1016/j.commatsci.2018.11.007.

References

[1] A.M. Kosevich, A.S. Kovalev, J. Sov. Phys. JETP 40 (1974) 891.
[2] A.S. Dolgov, Sov. Phys. Solid State 28 (1986) 907.
[3] A.J. Sievers, S. Takeno, Phys. Rev. Lett 61 (1988) 970.
[4] S. Flach, A.V. Gorbach, Phys. Rep. 467 (2008) 1.
[5] R. Hirota, J. Phys. Soc. Jpn. 35 (1973) 289.
[6] M.J. Ablowitz, J.F. Ladik, J. Math. Phys. 17 (1976) 1011.
[7] D. Cai, A.R. Bishop, N. Grønbech-Jensen, Phys. Rev. E 53 (1996) 4131.
[8] M.M. Bogdan, G.A. Maugin, Proc. Estonian Acad. Sci. Phys. Math. 52 (2003) 76.
[9] D.V. Laptev, Lett. Mater. 4 (2014) 241.
[10] M.M. Bogdan, D.V. Laptev, J. Phys. Soc. Jpn. 83 (2014) 064007.
[11] R.S. MacKay, S. Aubry, Nonlinearity 7 (1994) 1623.
[12] D. Bambusi, Nonlinearity 9 (1996) 433.
[13] R. Livi, M. Spicci, R.S. MacKay, Nonlinearity 10 (1997) 1421.
[14] Y.S. Kivshar, G.P. Agrawal, Optical Solitons: From Fibers to Photonic Crystals, Academic Press, New York, 2003.
[15] H.N. Chan, K.W. Chow, Commun. Nonlin. Sci. Num. Simul. 65 (2018) 185.
[16] E. Trias, J.J. Mazo, A. Brinkman, T.P. Orlando, Physica D 156 (2001) 98.
[17] A.V. Ustinov, Chaos 13 (2003) 716.
[18] S. Shige, K. Miyasaka, W. Shi, Y. Soga, M. Sato, A.J. Sievers, Europhys. Lett. 121 (2018) 30003.
[19] M. Sato, T. Mukaide, T. Nakaguchi, A.J. Sievers, Phys. Rev. E 94 (2016) 012223.
[20] M. Sato, B.E. Hubbard, A.J. Sievers, Rev. Mod. Phys. 78 (2006) 137.
[21] M. Kimura, Y. Matsushita, T. Hikihara, Phys. Lett. A 380 (2016) 2823.
[22] R.B. Thakur, L.Q. English, A.J. Sievers, J. Phys. D: Appl. Phys. 41 (2008) 015503.
[23] Y. Watanabe, T. Nishida, Y. Doi, N. Sugimoto, Phys. Lett. A 382 (2018) 1957.
[24] M.A. Porter, P.G. Kevrekidis, C. Daraio, Phys. Today 68 (2015) 44.
[25] D.K. Campbell, S. Flach, Yu.S. Kivshar, Phys. Today 57 (2004) 43.
[26] M. Manley, Acta Mater. 58 (2010) 2926.

[27] B.I. Swanson, J.A. Brozik, S.P. Love, G.F. Strouse, A.P. Shreve, A.R. Bishop, W.-Z. Wang, M.I. Salkola, Phys. Rev. Lett. 82 (1999) 3288.
[28] M.E. Manley, D.L. Abernathy, N.I. Agladze, A.J. Sievers, Sci. Rep. 1 (2011) 4.
[29] M.E. Manley, A.J. Sievers, J.W. Lynn, S.A. Kiselev, N.I. Agladze, Y. Chen, A. Llobet, A. Alatas, Phys. Rev. B 79 (2009) 134304.
[30] M.E. Manley, M. Yethiraj, H. Sinn, H.M. Volz, A. Alatas, J.C. Lashley, W.L. Hults, G.H. Lander, J.L. Smith, Phys. Rev. Lett. 96 (2006) 125501.
[31] M.E. Manley, A. Alatas, F. Trouw, B.M. Leu, J.W. Lynn, Y. Chen, W.L. Hults, Phys. Rev. B 77 (2008) 214305.
[32] M.E. Manley, J.W. Lynn, Y. Chen, G.H. Lander, Phys. Rev. B 77 (2008) 052301.
[33] S.V. Dmitriev, E.A. Korznikova, J.A. Baimova, M.G. Velarde, Phys. Usp. 59 (2016) 446.
[34] S.V. Dmitriev, Lett. Mater. 6 (2016) 86.
[35] J.A. Baimova, E.A. Korznikova, I.P. Lobzenko, S.V. Dmitriev, Rev. Adv. Mater. Sci. 42 (2015) 68.
[36] V.I. Dubinko, P.A. Selyshchev, J.F.R. Archilla, Phys. Rev. E 83 (2011) 041124.
[37] V.I. Dubinko, J.F.R. Archilla, S.V. Dmitriev, V. Hizhnyakov, Springer Series Mate 221 (2015) 381.
[38] V.I. Dubinko, D.V. Laptev, Lett. Mater. 6 (2016) 16.
[39] D. Xiong, D. Saadatmand, S.V. Dmitriev, Phys. Rev. E 96 (2017) 042109.
[40] M. Eleftheriou, S. Flach, Physica D 202 (2005) 142.
[41] L.Z. Khadeeva, S.V. Dmitriev, Phys. Rev. B 84 (2011) 144304.
[42] J.A. Baimova, R.T. Murzaev, A.I. Rudskoy, Phys. Lett. A 381 (2017) 3049.
[43] D.A. Terentyev, A.V. Dubinko, V.I. Dubinko, S.V. Dmitriev, E.E. Zhurkin, M.V. Sorokin, Model. Simul. Mater. Sci. Eng. 23 (2015) 085007.
[44] N.K. Voulgarakis, G. Hadjisavvas, P.C. Kelires, G.P. Tsironis, Phys. Rev. B 69 (2004) 113201.
[45] R.T. Murzaev, D.V. Bachurin, E.A. Korznikova, S.V. Dmitriev, Phys. Lett. A 381 (2017) 1003.
[46] V. Hizhnyakov, M. Haas, A. Pishtshev, A. Shelkan, M. Klopov, Nucl. Instrum. Meth. Phys. Res. B 303 (2013) 91.
[47] M. Haas, V. Hizhnyakov, A. Shelkan, M. Klopov, A.J. Sievers, Phys. Rev. B 84 (2011) 144303.
[48] R.T. Murzaev, A.A. Kistanov, V.I. Dubinko, D.A. Terentyev, S.V. Dmitriev, Comp. Mater. Sci. 98 (2015) 88.
[49] O.V. Bachurina, R.T. Murzaev, A.S. Semenov, E.A. Korznikova, S.V. Dmitriev, Phys. Solid State 60 (2018) 989.
[50] R.T. Murzaev, R.I. Babicheva, K. Zhou, E.A. Korznikova, S.Y. Fomin, V.I. Dubinko, S.V. Dmitriev, Eur. Phys. J. B 89 (2016) 168.
[51] P.V. Zakharov, M.D. Starostenkov, A.M. Eremin, E.A. Korznikova, S.V. Dmitriev, Phys. Solid State 59 (2017) 223.
[52] N.N. Medvedev, M.D. Starostenkov, P.V. Zakharov, S.V. Dmitriev, Tech. Phys. Lett. 41 (2015) 994.
[53] N.N. Medvedev, M.D. Starostenkov, P.V. Zakharov, O.V. Pozidaeva, Tech. Phys. Lett. 37 (2011) 98.
[54] S.A. Kiselev, A.J. Sievers, Phys. Rev. B 55 (1997) 5755.
[55] L.Z. Khadeeva, S.V. Dmitriev, Phys. Rev. B 81 (2010) 214306.
[56] A.A. Kistanov, S.V. Dmitriev, Tech. Phys. Lett. 39 (2013) 618.
[57] A.A. Kistanov, Y.A. Baimova, S.V. Dmitriev, Tech. Phys. Lett. 38 (2012) 676.
[58] I. Evazzade, I.P. Lobzenko, E.A. Korznikova, I.A. Ovid'ko, M.R. Roknabadi, S.V. Dmitriev, Phys. Rev. B 95 (2017) 035423.
[59] Y. Yamayose, Y. Kinoshita, Y. Doi, A. Nakatani, T. Kitamura, Europhys. Lett. 80 (2007) 40008.
[60] Y. Kinoshita, Y. Yamayose, Y. Doi, A. Nakatani, T. Kitamura, Phys. Rev. B 77 (2008) 024307.
[61] Y. Doi, A. Nakatani, Proc. Eng. 10 (2011) 3393.
[62] Y. Doi, A. Nakatani, Lett. Mater. 6 (2016) 49.
[63] L.Z. Khadeeva, S.V. Dmitriev, Y.S. Kivshar, JETP Lett. 94 (2011) 539.
[64] I. Evazzade, M.R. Roknabadi, M. Behdani, F. Moosavi, D. Xiong, K. Zhou, S.V. Dmitriev, Eur. Phys. J. B 91 (2018) 163.
[65] G.M. Chechin, S.V. Dmitriev, I.P. Lobzenko, D.S. Ryabov, Phys. Rev. B 90 (2014) 045432.
[66] I.P. Lobzenko, G.M. Chechin, G.S. Bezuglova, Y.A. Baimova, E.A. Korznikova, S.V. Dmitriev, Phys. Solid State 58 (2016) 633.
[67] LAMMPS Molecular Dynamics Simulator: < http://lammps.sandia.gov/ > .
[68] X.W. Zhou, J.A. Zimmerman, B.M. Wong, J.J. Hoyt, J. Mater. Res. 23 (2008) 704.
[69] J.E. Angelo, N.R. Moody, M.I. Baskes, Model. Simul. Mater. Sci. Eng. 3 (1995) 289.
[70] L.L. Kong, Comput. Phys. Commun. 182 (2011) 2201.
[71] V.I. Dubinko, D.V. Laptev, A.S. Mazmanishvili, J.F.R. Archilla, J. Micromech. Mol. Phys. 1 (2016) 1650010.
[72] V.I.J. Dubinko, Conden. Matter Nucl. Sci. 23 (2017) 45.
[73] V. Dubinko, D. Laptev, K. Irwin, J. Conden. Matter Nucl. Sci. 24 (2017) 1.